Hindawi Publishing Corporation
International Journal of Antennas and Propagation
Volume 2016, Article ID 6271648, 10 pages
http://dx.doi.org/10.1155/2016/6271648

Research Article

Transmit/Receive Spatial Smoothing with Improved Effective Array Aperture for Angle and Mutual Coupling Estimation in Bistatic MIMO Radar

Haomiao Liu, Xiaojun Yang, Rong Wang, Wei Jin, and Weimin Jia

Xi'an Research Institute of Hi-Tech, Xi'an 710025, China

Correspondence should be addressed to Xiaojun Yang; yxj029@163.com

Received 13 October 2015; Revised 16 December 2015; Accepted 21 December 2015

Academic Editor: Wei Liu

Copyright © 2016 Haomiao Liu et al. This is an open access article distributed under the Creative Commons Attribution License, which permits unrestricted use, distribution, and reproduction in any medium, provided the original work is properly cited.

We proposed a transmit/receive spatial smoothing with improved effective aperture approach for angle and mutual coupling estimation in bistatic MIMO radar. Firstly, the noise in each channel is restrained, by exploiting its independency, in both the spatial domain and temporal domain. Then the augmented transmit and receive spatial smoothing matrices with improved effective aperture are obtained, by exploiting the Vandermonde structure of steering vector with uniform linear array. The DOD and DOA can be estimated by utilizing the unitary ESPRIT algorithm. Finally, the mutual coupling coefficients of both the transmitter and the receiver can be figured out with the estimated angles of DOD and DOA. Numerical examples are presented to verify the effectiveness of the proposed method.

1. Introduction

A novel array radar named as multiple-input multiple-output (MIMO) radar has improved the progress of array signal processing [1, 2]. Because the MIMO radar is more flexible than the phased array radar [3], it has been researched in many fields [4]. In general, the MIMO radar can be divided into two classes: statistical MIMO radar and collocated MIMO radar. It is statistical MIMO radar where the transmit and receive antennas are widely distributed [5], which owns the spatial diversity. The transmit and receive antennas are closely located in collocated MIMO radar [6]. Because the antennas transmit totally or partially noncoherent waveforms in the transmitter, a virtual array with larger aperture in the receiver can be formed and higher resolution can be obtained for the waveform diversity. In this paper, we focus on the collocated MIMO radar.

The direction of departure (DOD) and direction of arrival (DOA) estimation are one of the most important aspects in bistatic MIMO radar with collocated antennas. And a lot of algorithms have been presented for this issue. In [7], the Capon based algorithm for DOD and DOA estimation in bistatic MIMO radar is presented. An estimation of signal parameters via rotational invariance technique (ESPRIT) method [8] is proposed by exploiting the invariance property of the transmit array and the receive array. The unitary ESPRIT algorithm for joint angles estimation is presented in [9], which has comparable angle estimation performance as ESPRIT with lower computational complexity. The multiple signal classification (MUSIC) is utilized for estimation of DOD and DOA in [10]. As the tensor is used widely in multidimensional signal processing, a three-dimensional tensor decomposition method, parallel factor (PARAFAC) analysis, is used to estimate DOD and DOA [11], which has a better performance than the other methods. There are a lot of methods for joint DOD and DOA estimation in bistatic MIMO radar, and we have just presented representative ones.

In recent years, although many institutes and researchers have been studying this novel radar, only a few of institutes have built up physical systems (e.g., the ONERA in France). In [12], it points out that the mutual coupling is a major cause of descending the performance of radar by real data experiment. In order to eliminate the effect of mutual coupling, a MUSIC-Like method is proposed in [13], and the mutual coupling coefficients can be estimated. But this method loses partial effective aperture and it needs lots of snapshots for

performance guarantee. In [14], an ESPRIT-Like method performs better than MUSIC-Like method. However, in the case of small snapshots, the accuracy of angle estimation using both of the above approaches will degrade remarkably. By exploiting the multidimensional structure of the received data, a three-order tensor is constructed [15], which are DOD, DOA, and temporal dimensions, respectively. And a real-valued subspace approach is proposed; it computes the subspace utilizing the higher order singular value decomposition (HOSVD). Due to use of the forward-backward averaging technique, this approach is suitable for coherent targets and small snapshots. However, the tensor-based real-valued subspace approach just employs partial aperture; it loses a lot of information. When there exists coherent targets, the performance of that approach will degrade, and it cannot deal with more than two coherent targets. Spatial smoothing technique is an effective approach to deal with the situation of small snapshots and coherent targets. In [16], a spatial smoothing with improved aperture (SSIA) method is proposed to estimate DOA for the phased array radar; it improves the effective array aperture twice larger than the conventional spatial smoothing approaches. This technique also can be used to estimate DOD and DOA for bistatic MIMO radar.

In this paper, we proposed a transmit/receive spatial smoothing with improved effective aperture (TRSSIA) method for joint DOD and DOA estimation in bistatic MIMO radar with unknown mutual coupling. Firstly, the white Gaussian noise is restrained using its dependency in both the spatial and temporal domains. Then the TRSSIA is used to construct the transmit spatial smoothing matrix and the receive spatial smoothing matrix. Due to the Vandermonde structure of steering vector with uniform linear arrays (ULA), the transmit and receive augmented spatial smoothing matrices are constructed, and these two matrices can improve the effective aperture two times larger than conventional ones. Thirdly, by using the centro-Hermitian structure of augmented matrices, the real-valued subspace methods (e.g., unitary ESPRIT) can be used to estimate DOD and DOA. Finally, an additional DOD and DOA pairing technique is proposed and the mutual coupling coefficients are estimated. The proposed approach restrains white Gaussian noise and takes full advantage of the received data, so it provides better angle estimation performance. And it can deal with more than two coherent targets.

The remainder of the paper is organized as follows. In Section 2, the bistatic MIMO radar signal model is introduced. The coupling calibration approach is demonstrated in Section 3. In Section 4, simulations are employed to verify the analytical derivations. Finally, Section 5 gives the conclusion.

Notation. $(\cdot)^{\mathrm{H}}, (\cdot)^{\mathrm{T}}, (\cdot)^{-1}$, and $(\cdot)^{*}$ denote conjugate transpose, transpose, inverse, and conjugate, respectively. $\otimes$ and $\odot$ denote the Kronecker product operation and Khatri-Rao product operation. Toeplitz($\mathbf{c}$) denotes the symmetric Toeplitz matrix constructed by the vector $\mathbf{c}$. diag$(\cdot)$ denotes the diagonalization operation. mat$(\cdot)$ denotes the matrixing operation. Re$\{\cdot\}$ and Im$\{\cdot\}$ denote abstracting the real part and imaginary part of complex number, respectively. $\mathbf{e}_{\min}(\cdot)$ is an operator of getting the minimum eigenvector. mean$(\cdot)$ is used to compute the mean of numbers. $\mathbf{I}_M$ denotes the $M\times$M identity matrix, and $\mathbf{0}_{M\times N}$ is the $M\times N$ zero matrix. $\mathbf{A}[i:j,:]$ denotes the ith to the jth rows of $\mathbf{A}$.

2. Bistatic MIMO Radar Signal Model

Consider a bistatic MIMO radar system equipped with M transmit antennas and N receive antennas, both of which are ULA with half-wavelength spacing antennas. The transmit antennas emit M orthogonal waveforms $\widetilde{\mathbf{S}} = [\widetilde{\mathbf{s}}_1, \widetilde{\mathbf{s}}_2, \ldots, \widetilde{\mathbf{s}}_M]^{\mathrm{T}}$, and $\widetilde{\mathbf{S}}\widetilde{\mathbf{S}}^{\mathrm{H}}/K = \mathbf{I}_M$, where K is the number of samples per pulse period. All the targets are modeled as point-scatters in the far-field, and we assume that there exists P targets in the same range bin. Consider the effect of mutual coupling in both the transmitter and receiver; the received data of the lth pulse is shown as

$$\mathbf{X}(l) = [\mathbf{C}_r\mathbf{A}_r]\,\mathbf{\Lambda}(l)\,[\mathbf{C}_t\mathbf{A}_t]^{\mathrm{T}}\,\widetilde{\mathbf{S}} + \mathbf{W}(l), \quad l = 1, 2, \ldots, L, \tag{1}$$

where $\mathbf{X}(l) \in \mathbb{C}^{N\times K}$ is the received data during the lth pulse period and L is the number of pulses. $\mathbf{C}_t$ and $\mathbf{C}_r$ are the mutual coupling matrices of the transmit and receive arrays, respectively, which can be expressed as banded symmetric Toeplitz matrices [17]:

$$\mathbf{C}_t = \text{toeplitz}\left\{\left[1, c_{t1}, \ldots, c_{tp_t}, 0, \ldots, 0\right]\right\} \in \mathbb{C}^{M\times M}, \tag{2a}$$

$$\mathbf{C}_r = \text{toeplitz}\left\{\left[1, c_{r1}, \ldots, c_{rp_r}, 0, \ldots, 0\right]\right\} \in \mathbb{C}^{N\times N}, \tag{2b}$$

where c_{ti}, c_{rj} are the transmit and receive mutual coupling coefficients and there are p_t and p_r nonzero mutual coupling coefficients with $M \geq 2p_t + 1$, $N \geq 2p_r + 1$, respectively. $\mathbf{A}_t = [\mathbf{a}_{t_1}, \mathbf{a}_{t_2}, \ldots, \mathbf{a}_{t_P}]$, $\mathbf{A}_r = [\mathbf{a}_{r_1}, \mathbf{a}_{r_2}, \ldots, \mathbf{a}_{r_P}]$, $\mathbf{a}_{t_p} = [1, \exp(\mathrm{j}2\pi d_t \sin\phi_p/\lambda), \ldots, \exp(\mathrm{j}2\pi(M-1)d_t\sin\phi_p/\lambda)]^{\mathrm{T}}$, and $\mathbf{a}_{r_p} = [1, \exp(\mathrm{j}2\pi d_r \sin\theta_p/\lambda), \ldots, \exp(\mathrm{j}2\pi(N-1)d_r\sin\theta_p/\lambda)]^{\mathrm{T}}$ are the receive steering vector and the transmit steering vector, where d_t and d_r are the adjacent antenna spacing of transmit and receive arrays, respectively. ϕ_p and θ_p are DOD and DOA of the pth target and λ denoting the wavelength. One has $\mathbf{\Lambda}(l) = \text{diag}([s_1(l), s_2(l), \ldots, s_P(l)])$, where $s_p(l) = \beta_p \exp(\mathrm{j}2\pi f_p l)$ is the reflected signal of the pth target and β_p and f_p are the amplitude and Doppler frequency, respectively. $\mathbf{W}(l) \in \mathbb{C}^{N\times K}$ is the complex white Gaussian noise matrix, with the covariance $\delta_w^2\mathbf{I}_N$ [18, 19]. After matched filtering, the output data at the receiver can be expressed as

$$\mathbf{x}(l) = \mathbf{CAs}(l) + \mathbf{w}(l), \tag{3}$$

where $\mathbf{C} = \mathbf{C}_t \otimes \mathbf{C}_r$, $\mathbf{A} = \mathbf{A}_t \odot \mathbf{A}_r$, $\mathbf{s}(l) = [s_1(l), s_2(l), \ldots, s_P(l)]^{\mathrm{T}}$, $\mathbf{w}(l) = \text{vec}(\mathbf{W}(l)\widetilde{\mathbf{S}}^{\mathrm{H}}/K)$.

It assumes that the noise is i.i.d. complex white Gaussian noise, and we can obtain the equation written as

$E[\mathrm{vec}(\mathbf{W}(l))\mathrm{vec}^{\mathrm{H}}(\mathbf{W}(l))] = \mathbf{I}_K \otimes \delta_w^2 \mathbf{I}_N$. Furthermore, according to the properties of Kronecker product [20, 21], we can obtain the following equation:

$$\begin{aligned} E\left[\mathbf{w}(l)\,\mathbf{w}(l)^{\mathrm{H}}\right] &= \frac{E\left[\mathrm{vec}\left(\mathbf{W}(l)\,\widetilde{\mathbf{S}}^{\mathrm{H}}\right)\mathrm{vec}^{\mathrm{H}}\left(\mathbf{W}(l)\,\widetilde{\mathbf{S}}^{\mathrm{H}}\right)\right]}{K^2} \\ &= \frac{E\left[\left(\widetilde{\mathbf{S}}^{*}\otimes\mathbf{I}_N\right)\left(\mathrm{vec}\left(\mathbf{W}(l)\right)\mathrm{vec}^{\mathrm{H}}\left(\mathbf{W}(l)\right)\right)\left(\widetilde{\mathbf{S}}^{\mathrm{T}}\otimes\mathbf{I}_N\right)\right]}{K^2} \\ &= \frac{\left(\widetilde{\mathbf{S}}^{*}\otimes\mathbf{I}_N\right)\left(\mathbf{I}_K\otimes\delta_w^2\mathbf{I}_N\right)\left(\widetilde{\mathbf{S}}^{\mathrm{T}}\otimes\mathbf{I}_N\right)}{K^2} = \frac{\mathbf{I}_M\otimes\delta_w^2\mathbf{I}_N}{K} \\ &= \frac{\delta_w^2\mathbf{I}_{MN}}{K}. \end{aligned} \tag{4}$$

3. Proposed Algorithm

3.1. Restraining Noise. According to (4), the noise of all MN channels are independent. Meanwhile, the noise of each channel is also independent in the temporal domain. So we can restrain the noise both in the spatial and temporal domain. For the ULA, the received data of each channel is expressed as

$$x_{m,n}(l) = \sum_{p=1}^{P} a_{t_p m} a_{r_p n} s_p(l) + w_{m,n}(l), \tag{5}$$

where $x_{m,n}(l)$ means the $(m-1)N+n$th row of $\mathbf{x}(l)$, $w_{m,n}(l)$ is the $(m-1)N+n$th row of $\mathbf{w}(l)$,and $a_{t_p m}$ and $a_{r_p n}$ are the mth element and the nth element of $\mathbf{a}_{t_p}$ and $\mathbf{a}_{r_p}$, respectively. When $m=1$, $n=1$, $x_{1,1}(l) = \sum_{p=1}^{P} s_p(l) + w_{1,1}(l)$, the correlation coefficient can be expressed as

$$\begin{aligned} r_{(1,1),(1,1)}(\Delta l) &= E\left[x_{1,1}(l)\,x_{1,1}^{*}(l+\Delta l)\right] \\ &= \sum_{p_1=1}^{P}\sum_{p_2=1}^{P}\sigma_{(p_1,p_2)}^2, \end{aligned} \tag{6}$$

where $\sigma_{(p_1,p_2)}^2$ is the correlation coefficient between $s_{p_1}(l)$ and $s_{p_2}(l+\Delta l)$. For the white Gaussian noise, the correlation coefficient of two adjacent noises and the correlation coefficient of signal and noise are both zeros in the temporal domain. And in the spatial domain, we can get the correlation efficient between any channel and the first channel which can be shown as

$$\begin{aligned} r_{(m,n),(1,1)}(\Delta l) &= E\left[x_{m,n}(l)\,x_{1,1}^{*}(l+\Delta l)\right] \\ &= \sum_{p_1=1}^{P} a_{t_{p_1} m} a_{r_{p_1} n} \sum_{p_2=1}^{P}\sigma_{(p_1,p_2)}^2. \end{aligned} \tag{7}$$

As we known from (4), the noise is independent in spatial domain. So the correlation coefficient of noise between any channel and the first channel equals zero.

Factually, we can only get limited snapshots, so we obtain the asymptotic correlation coefficients:

$$\begin{aligned} \widehat{r}_{(1,1),(1,1)}(\Delta l) &= \sum_{l={}'l}^{{}'l+L}\frac{x_{1,1}(l)\,x_{1,1}^{*}(l+\Delta l)}{L} \\ &= \sum_{p_1=1}^{P}\sum_{p_2=1}^{P}\widehat{\sigma}_{(p_1,p_2)}^2 + \widehat{\varepsilon}_{(1,1)}^2, \end{aligned} \tag{8a}$$

$$\begin{aligned} \widehat{r}_{(m,n),(1,1)}(\Delta l) &= \sum_{l={}'l}^{{}'l+L}\frac{x_{m,n}(l)\,x_{1,1}^{*}(l+\Delta l)}{L} \\ &= \sum_{p_1=1}^{P} a_{t_{p_1} m} a_{r_{p_1} n} \sum_{p_2=1}^{P}\widehat{\sigma}_{(p_1,p_2)}^2 + \widehat{\varepsilon}_{(m,n)}^2, \end{aligned} \tag{8b}$$

where $\widehat{\varepsilon}_{(1,1)}^2$ and $\widehat{\varepsilon}_{(m,n)}^2$ are the correlation coefficients of noise, which nearly equal zeros.

According to (8a)-(8b), we obtain a new vector, which can be written as

$$\begin{aligned} &\widehat{\mathbf{r}}(\Delta l) \\ &= \left[\widehat{r}_{(1,1),(1,1)}(\Delta l), \widehat{r}_{(1,2),(1,1)}(\Delta l), \ldots, \widehat{r}_{(M,N),(1,1)}(\Delta l)\right]^{\mathrm{T}} \\ &= \mathbf{A}_t \odot \mathbf{A}_r \rho + \mathbf{v}, \end{aligned} \tag{9}$$

where $\rho = [\sum_{p_2=1}^{P}\widehat{\sigma}_{(1,p_2)}^2, \sum_{p_2=1}^{P}\widehat{\sigma}_{(2,p_2)}^2, \ldots, \sum_{p_2=1}^{P}\widehat{\sigma}_{(P,p_2)}^2]^{\mathrm{T}}$, $\mathbf{v} = [\widehat{\varepsilon}_{(1,1)}^2, \widehat{\varepsilon}_{(1,2)}^2, \ldots, \widehat{\varepsilon}_{(M,N)}^2]^{\mathrm{T}}$.

Consider the effect of mutual coupling in both the transmitter and receiver; we construct two selection matrices:

$$\mathbf{J}_t = \mathbf{J}_1 \otimes \mathbf{I}_N \quad \mathbf{J}_1 = \left[\mathbf{0}_{(M-2p_t)\times p_t}, \mathbf{I}_{M-2p_t}, \mathbf{0}_{(M-2p_t)\times p_t}\right], \tag{10a}$$

$$\mathbf{J}_r = \mathbf{I}_M \otimes \mathbf{J}_2 \quad \mathbf{J}_2 = \left[\mathbf{0}_{(N-2p_r)\times p_r}, \mathbf{I}_{N-2p_r}, \mathbf{0}_{(N-2p_r)\times p_r}\right]. \tag{10b}$$

Then we use these two selection matrices on the received data; it can get the selected data:

$$\begin{aligned} \mathbf{x}_t(l) &= \mathbf{J}_t\mathbf{x}(l) = \left[\mathbf{J}_1\mathbf{C}_t\mathbf{A}_t\right]\odot\left[\mathbf{C}_r\mathbf{A}_r\right]\mathbf{s}(l) + \mathbf{J}_t\mathbf{w}(l) \\ &= \overline{\mathbf{A}}_t \odot \widetilde{\mathbf{A}}_r\overline{\mathbf{s}}(l) + \overline{\mathbf{w}}(l), \end{aligned} \tag{11}$$

where $\overline{\mathbf{A}}_t$ is the first $M-2p_t$ rows of $\mathbf{A}_t$, $\widetilde{\mathbf{A}}_r = [\mathbf{C}_r\mathbf{A}_r]\mathrm{diag}(\mathbf{C}_r(1,:)\mathbf{A}_r)^{-1}$, and $\overline{\mathbf{s}}(l) = [\overline{s}_1(l), \overline{s}_2(l), \ldots, \overline{s}_P(l)]^{\mathrm{T}}$, $\overline{s}_p(l) = \tau_p\mathbf{C}_r(1,:)\mathbf{a}_{rp}s_p(l)$, $\tau_p = \sum_{q=-p_t}^{p_t} c_{t|q|}e^{j\pi(q+p_t)\sin\phi_p}$. Meanwhile, we can get another selected data vector, which can be expressed as

$$\begin{aligned} \mathbf{x}_r(l) &= \mathbf{J}_r\mathbf{x}(l) = \left[\mathbf{C}_t\mathbf{A}_t\right]\odot\left[\mathbf{J}_2\mathbf{C}_r\mathbf{A}_r\right]\mathbf{s}(l) + \mathbf{J}_r\mathbf{w}(l) \\ &= \widetilde{\mathbf{A}}_t \odot \overline{\mathbf{A}}_r\widetilde{\mathbf{s}}(l) + \widetilde{\mathbf{w}}(l), \end{aligned} \tag{12}$$

where $\overline{\mathbf{A}}_r$ is the first $N-2p_r$ rows of $\mathbf{A}_r$, $\widetilde{\mathbf{A}}_t = [\mathbf{C}_t\mathbf{A}_t]\mathrm{diag}(\mathbf{C}_t(1,:)\mathbf{A}_t)^{-1}$, and $\widetilde{\mathbf{s}}(l) = [\widetilde{s}_1(l), \widetilde{s}_2(l), \ldots, \widetilde{s}_P(l)]^{\mathrm{T}}$, $\widetilde{s}_p(l) = \gamma_p\mathbf{C}_t(1,:)\mathbf{a}_{tp}s_p(l)$, $\gamma_p = \sum_{q=-p_r}^{p_r} c_{r|q|}e^{j\pi(q+p_r)\sin\theta_p}$. The selected noise vectors $\overline{\mathbf{w}}$ and $\widetilde{\mathbf{w}}$ are both white Gaussian.

Then we restrain the noise of selected data, based on (8a)-(8b). It obtains two received vectors, which are shown as

$$\begin{aligned}\widehat{\mathbf{r}}_t(\Delta l) = \big[&\widehat{r}_{t(1,1),(1,1)}(\Delta l), \widehat{r}_{t(1,2),(1,1)}(\Delta l), \ldots, \\ &\widehat{r}_{t(M1,N),(1,1)}(\Delta l)\big]^{\mathrm{T}} = \overline{\mathbf{A}}_t \odot \widetilde{\mathbf{A}}_r \widehat{\rho}_t + \widehat{\mathbf{v}}_t,\end{aligned} \tag{13a}$$

$$\begin{aligned}\widehat{\mathbf{r}}_r(\Delta l) = \big[&\widehat{r}_{r(1,1),(1,1)}(\Delta l), \widehat{r}_{r(1,2),(1,1)}(\Delta l), \ldots, \\ &\widehat{r}_{r(M,N1),(1,1)}(\Delta l)\big]^{\mathrm{T}} = \widetilde{\mathbf{A}}_t \odot \overline{\mathbf{A}}_r \widehat{\rho}_r + \widehat{\mathbf{v}}_r,\end{aligned} \tag{13b}$$

where $M1 = M - 2p_t$, $N1 = N - 2p_r$, $\widehat{\rho}_t = [\sum_{p_2=1}^{P} \widehat{\sigma}^2_{t(1,p_2)}, \sum_{p_2=1}^{P} \widehat{\sigma}^2_{t(2,p_2)}, \ldots, \sum_{p_2=1}^{P} \widehat{\sigma}^2_{t(P,p_2)}]^{\mathrm{T}}$, $\widehat{\rho}_r = [\sum_{p_2=1}^{P} \widehat{\sigma}^2_{r(1,p_2)}, \sum_{p_2=1}^{P} \widehat{\sigma}^2_{r(2,p_2)}, \ldots, \sum_{p_2=1}^{P} \widehat{\sigma}^2_{r(P,p_2)}]^{\mathrm{T}}$, and $\widehat{\sigma}^2_{t(i,p_2)}$, $\widehat{\sigma}^2_{r(j,p_2)}$ are the correlation coefficients of $\overline{s}_i(l)$ and $\overline{s}_{p_2}(l)$ and the correlation coefficient of $\widetilde{s}_j(l)$ and $\widetilde{s}_{p_2}(l)$, respectively. $\widehat{\mathbf{v}}_t = [\widehat{\varepsilon}^2_{t(1,1)}, \widehat{\varepsilon}^2_{t(1,2)}, \ldots, \widehat{\varepsilon}^2_{t(M1,N)}]^{\mathrm{T}}$ and $\widehat{\mathbf{v}}_r = [\widehat{\varepsilon}^2_{r(1,1)}, \widehat{\varepsilon}^2_{r(1,2)}, \ldots, \widehat{\varepsilon}^2_{r(M,N1)}]^{\mathrm{T}}$, where $\widehat{\varepsilon}^2_{t(m,n)}$ and $\widehat{\varepsilon}^2_{r(m,n)}$ are the correlation coefficients of $\overline{\mathbf{w}}_{t,(1,1)}(l)$ and $\overline{\mathbf{w}}_{t,(m,n)}(l + \Delta l)$, $\widetilde{\mathbf{w}}_{r,(1,1)}(l)$, and $\widetilde{\mathbf{w}}_{r,(m,n)}(l + \Delta l)$, respectively.

3.2. Transmit/Receive Spatial Smoothing with Improved Aperture. After restraining the noise, we obtain the new received data vector $\widehat{\mathbf{r}}_t(\Delta l)$, $\widehat{\mathbf{r}}_r(\Delta l)$. In the following, we omit Δl and write the received data as $\widehat{\mathbf{r}}_t$, $\widehat{\mathbf{r}}_r$. In [16], a spatial smoothing with improved aperture (SSIA) method with single snapshot is proposed. It is suitable for coherent sources and improves the effective aperture. This approach performs well for DOA estimation in the phased array radar. In this paper, it will prove that this technique can work well in the MIMO radar.

Firstly, we define a $m \times m$ exchange matrix $\mathbf{\Pi}_m$ with ones on its antidiagonal and zeros elsewhere. Then, the left-$\mathbf{\Pi}$-real matrix $\mathbf{Q}$ can be expressed as [22]

$$\mathbf{Q}_{2n+1} = \frac{1}{\sqrt{2}} \begin{bmatrix} \mathbf{I}_n & \mathbf{0} & \mathrm{j}\mathbf{I}_n \\ \mathbf{0}^{\mathrm{T}} & \sqrt{2} & \mathbf{0}^{\mathrm{T}} \\ \mathbf{\Pi}_n & \mathbf{0} & -\mathrm{j}\mathbf{\Pi}_n \end{bmatrix}. \tag{14}$$

Equation (14) is a left-$\mathbf{\Pi}$-real matrix of odd order. The $2n$ order one is obtained from $\mathbf{Q}_{2n+1}$ by dropping the center row and center column.

For $\widehat{\mathbf{r}}_t$ and $M1 = M_{\mathrm{sub}} + L_t - 1$, we define

$$\begin{aligned}&\widehat{\mathbf{X}}_t \\ &= \left[(\mathbf{H}_{t1} \otimes \mathbf{I}_{\mathrm{N}})\widehat{\mathbf{r}}_t, (\mathbf{H}_{t2} \otimes \mathbf{I}_N)\widehat{\mathbf{r}}_t, \ldots, (\mathbf{H}_{tL_t} \otimes \mathbf{I}_N)\widehat{\mathbf{r}}_t\right], \\ &\mathbf{H}_{tl} = \left[\mathbf{0}_{M_{\mathrm{sub}} \times (l-1)}, \mathbf{I}_{M_{\mathrm{sub}}}, \mathbf{0}_{M_{\mathrm{sub}} \times (L_t - l)}\right], \quad 1 \le l \le L_t.\end{aligned} \tag{15}$$

And (15) can be expressed as

$$\widehat{\mathbf{X}}_t = \left[\dot{\mathbf{A}}_t \odot \widetilde{\mathbf{A}}_r\right] \widehat{\mathbf{\Lambda}}_t \ddot{\mathbf{A}}_t^{\mathrm{T}} + \widehat{\mathbf{V}}_t, \tag{16}$$

where $\widehat{\mathbf{\Lambda}}_t = \mathrm{diag}(\widehat{\rho}_t)$, $\dot{\mathbf{A}}_t$ and $\ddot{\mathbf{A}}_t$ are the first M_{sub} rows and the first L_t rows of $\mathbf{A}_t$, respectively.

Then we obtain an augmented matrix:

$$\begin{aligned}\widehat{\mathbf{X}}_{\mathrm{taug}} &= \begin{bmatrix} \widehat{\mathbf{X}}_t \\ \mathbf{\Pi}_{M_{\mathrm{sub}}N} \widehat{\mathbf{X}}_t^* \mathbf{\Pi}_{L_t} \end{bmatrix} \\ &= \begin{bmatrix} \dot{\mathbf{A}}_t \odot \widetilde{\mathbf{A}}_r \widehat{\mathbf{\Lambda}}_t \\ \dot{\mathbf{A}}_t \odot \left(\mathbf{\Pi}_N \widetilde{\mathbf{A}}_r^*\right) \mathbf{\Lambda}_{t1} \widehat{\mathbf{\Lambda}}_t^* \mathbf{\Lambda}_{t2} \end{bmatrix} \ddot{\mathbf{A}}_t^{\mathrm{T}} \\ &\quad + \begin{bmatrix} \widehat{\mathbf{V}}_t \\ \mathbf{\Pi}_{M_{\mathrm{sub}}N} \widehat{\mathbf{V}}_t^* \mathbf{\Pi}_{L_t} \end{bmatrix} = \mathbf{A}_{\mathrm{taug}} \ddot{\mathbf{A}}_t^{\mathrm{T}} + \widehat{\mathbf{V}}_{\mathrm{taug}} \\ &\in \mathbb{C}^{2M_{\mathrm{sub}}N \times L_t},\end{aligned} \tag{17}$$

where $\mathbf{\Lambda}_{t1} = \mathrm{diag}([a_{t_1(1-M_{\mathrm{sub}})}, a_{t_2(1-M_{\mathrm{sub}})}, \ldots, a_{t_p(1-M_{\mathrm{sub}})}])$ and $\mathbf{\Lambda}_{t2} = \mathrm{diag}([a_{t_1(1-L_t)}, a_{t_2(1-L_t)}, \ldots, a_{t_p(1-L_t)}])$. The steering matrix $\mathbf{A}_{\mathrm{taug}}$ is twice larger than $\dot{\mathbf{A}}_t \odot \widetilde{\mathbf{A}}_r$. Although the noise matrix $\widehat{\mathbf{V}}_t$ is not white Gaussian, its effect on $\widehat{\mathbf{X}}_{\mathrm{taug}}$ is weak, as every element nearly equals zero. See Appendix for a brief illustration of the rotational invariance property of $\widehat{\mathbf{X}}_{\mathrm{taug}}$. The subspace approaches, such as MUSIC and ESPRIT, can be used to estimate DOD.

We note that $\widehat{\mathbf{X}}_{\mathrm{taug}}$ is a centro-Hermitian matrix, it satisfies the following identity:

$$\mathbf{\Pi}_{2M_{\mathrm{sub}}N} \widehat{\mathbf{X}}_{\mathrm{taug}}^* \mathbf{\Pi}_{L_t} = \widehat{\mathbf{X}}_{\mathrm{taug}}. \tag{18}$$

So the real-valued space methods, for example, unitary MUSIC and unitary ESPRIT, are suitable for $\widehat{\mathbf{X}}_{\mathrm{taug}}$ to estimate angles. In this paper, we estimate angles by utilizing the unitary ESPRIT algorithm. Then the complex matrix can be transformed into real-valued matrix as follows:

$$\varphi\left(\widehat{\mathbf{X}}_{\mathrm{taug}}\right) = \mathbf{Q}^{\mathrm{H}}_{2M_{\mathrm{sub}}N} \widehat{\mathbf{X}}_{\mathrm{taug}} \mathbf{Q}_{L_t}. \tag{19}$$

The real-valued signal subspace can be obtained by making SVD on $\varphi(\widehat{\mathbf{X}}_{\mathrm{taug}})$. The property of rotational invariance in real-valued subspace is shown as

$$\mathbf{K}^{(1)}_{\mathrm{taug}} \mathbf{E}_{\mathrm{taug}} \mathbf{\Upsilon}_{\mathrm{taug}} \approx \mathbf{K}^{(2)}_{\mathrm{taug}} \mathbf{E}_{\mathrm{taug}}, \tag{20}$$

where $\mathbf{E}_{\mathrm{taug}}$ contains the P dominant left singular vectors of $\varphi(\widehat{\mathbf{X}}_{\mathrm{taug}})$. Meanwhile, $\mathbf{K}^{(1)}_{\mathrm{taug}}$ and $\mathbf{K}^{(2)}_{\mathrm{taug}}$ are the transformed selection matrices; they are both obtained from $\mathbf{J}^{(2)}_{\mathrm{taug}}$ in the following way:

$$\mathbf{K}^{(1)}_{\mathrm{taug}} = 2 \cdot \mathrm{Re}\left\{\mathbf{Q}^{\mathrm{H}}_{2(M_{\mathrm{sub}}-1)N} \mathbf{J}^{(2)}_{\mathrm{taug}} \mathbf{Q}_{2M_{\mathrm{sub}}N}\right\}, \tag{21a}$$

$$\mathbf{K}^{(2)}_{\mathrm{taug}} = 2 \cdot \mathrm{Im}\left\{\mathbf{Q}^{\mathrm{H}}_{2(M_{\mathrm{sub}}-1)N} \mathbf{J}^{(2)}_{\mathrm{taug}} \mathbf{Q}_{2M_{\mathrm{sub}}N}\right\}, \tag{21b}$$

where $\mathbf{J}^{(2)}_{\mathrm{taug}} = \mathbf{I}_2 \otimes \mathbf{J}_{t2}$, $\mathbf{J}_{t2} = [\mathbf{0}_{(M_{\mathrm{sub}}-1)N \times N}, \mathbf{I}_{(M_{\mathrm{sub}}-1)N}]$.

A class of least squares (LS) approaches [20], for example, structured least squares (SLS) and total least squares (TLS), can be used to solve (20) for $\mathbf{\Upsilon}_{\mathrm{taug}}$. Ultimately, the angles of DOD can be figured out by $\{\phi_i\}_{i=1}^{P} = \mathrm{asin}(2\mathrm{atan}(\mathrm{eig}(\mathbf{\Upsilon}_{\mathrm{taug}}))/\pi)$.

In the same way, we estimate the angles of DOA. Firstly, for $N1 = N_{\text{sub}} + L_r - 1$, we obtain the augmented matrix:

$$\widehat{\mathbf{X}}_{\text{raug}} = \left[\widehat{\mathbf{X}}_r; \mathbf{\Pi}_{MN_{\text{sub}}} \widehat{\mathbf{X}}_r^* \mathbf{\Pi}_{L_r}\right] = \mathbf{A}_{\text{raug}} \ddot{\mathbf{A}}_r^{\text{T}} + \widehat{\mathbf{V}}_{\text{raug}} \in \mathbb{C}^{2MN_{\text{sub}} \times L_r}, \tag{22}$$

where $\widehat{\mathbf{X}}_r = [(\mathbf{I}_M \otimes \mathbf{H}_{r1})\widehat{\mathbf{r}}_r, (\mathbf{I}_M \otimes \mathbf{H}_{r2})\widehat{\mathbf{r}}_r, \ldots, (\mathbf{I}_M \otimes \mathbf{H}_{rL_r})\widehat{\mathbf{r}}_r]$ and $\mathbf{H}_{rl} = [\mathbf{0}_{N_{\text{sub}} \times (l-1)}, \mathbf{I}_{N_{\text{sub}}}, \mathbf{0}_{N_{\text{sub}} \times (L_r - l)}]$, $1 \le l \le L_r$. Furthermore, the augmented matrix can be exchanged into real-valued matrix $\varphi(\widehat{\mathbf{X}}_{\text{raug}}) = \mathbf{Q}_{2MN_{\text{sub}}}^{\text{H}} \widehat{\mathbf{X}}_{\text{raug}} \mathbf{Q}_{L_r}$. The real-valued signal subspace $\mathbf{E}_{\text{raug}}$ can be got by utilizing SVD on $\varphi(\widehat{\mathbf{X}}_{\text{raug}})$, and it meets the following relationship:

$$\mathbf{K}_{\text{raug}}^{(1)} \mathbf{E}_{\text{raug}} \mathbf{\Upsilon}_{\text{raug}} \approx \mathbf{K}_{\text{raug}}^{(2)} \mathbf{E}_{\text{raug}}, \tag{23}$$

where the selection matrices $\mathbf{K}_{\text{raug}}^{(1)}, \mathbf{K}_{\text{raug}}^{(2)}$ are constructed as $\mathbf{K}_{\text{raug}}^{(1)} = 2 \cdot \text{Re}\{\mathbf{Q}_{2M(N_{\text{sub}}-1)}^{\text{H}} \mathbf{J}_{\text{raug}}^{(2)} \mathbf{Q}_{2MN_{\text{sub}}}\}$, $\mathbf{K}_{\text{raug}}^{(2)} = 2 \cdot \text{Im}\{\mathbf{Q}_{2M(N_{\text{sub}}-1)}^{\text{H}} \mathbf{J}_{\text{raug}}^{(2)} \mathbf{Q}_{2MN_{\text{sub}}}\}$, and $\mathbf{J}_{\text{raug}}^{(2)} = \mathbf{I}_2 \otimes \mathbf{J}_{r2}$, $\mathbf{J}_{r2} = \mathbf{I}_M \otimes [\mathbf{0}_{(N_{\text{sub}}-1)\times 1} \quad \mathbf{I}_{N_{\text{sub}}-1}]$. Then the angles of DOA can be given by $\{\theta_j\}_{j=1}^P = \text{asin}(2\text{atan}(\text{eig}(\mathbf{\Upsilon}_{\text{raug}}))/\pi)$.

3.3. Pairing DOD and DOA. Because the proposed TRSSIA approach tries to make full use of the received data, the angles of DOD and DOA are figured out from transmit augmented matrix and receive augmented matrix, respectively. By exploiting the relationship between the steering vectors $\mathbf{a}_t, \mathbf{a}_r$ and the signal subspace $\mathbf{E}_{\text{taug}}, \mathbf{E}_{\text{raug}}$, then $\{\phi_i\}_{i=1}^P$ can be paired with $\{\theta_j\}_{j=1}^P$ correctly. Note that their relationship can be expressed as

$$\dot{\mathbf{A}}_t \odot \overline{\mathbf{A}}_r \mathbf{T}_1 = \mathbf{J}_{\text{taug}}^{(3)} \left(\mathbf{Q}_{2M_{\text{sub}}N} \mathbf{E}_{\text{taug}}\right) = \mathbf{U}_1, \tag{24a}$$

$$\overline{\mathbf{A}}_t \odot \dot{\mathbf{A}}_r \mathbf{T}_2 = \mathbf{J}_{\text{raug}}^{(3)} \left(\mathbf{Q}_{2MN_{\text{sub}}} \mathbf{E}_{\text{raug}}\right) = \mathbf{U}_2, \tag{24b}$$

where $\overline{\mathbf{A}}_t, \overline{\mathbf{A}}_r$ are the first $M1$ and $N1$ rows of $\mathbf{A}_t$ and $\mathbf{A}_r$ and $\mathbf{T}_1$ and $\mathbf{T}_2$ are both $P \times P$ nonsingular matrices. The selection matrices abstract parts of signal subspace are shown as

$$\mathbf{J}_{\text{taug}}^{(3)} = [1 \quad 0] \otimes \mathbf{J}_{t3}, \quad \mathbf{J}_{t3} = \mathbf{I}_{M_{\text{sub}}} \otimes [\mathbf{0}_{N1 \times p_r} \quad \mathbf{I}_{N1} \quad \mathbf{0}_{N1 \times p_r}], \tag{25a}$$

$$\mathbf{J}_{\text{raug}}^{(3)} = [1 \quad 0] \otimes \mathbf{J}_{r3}, \quad \mathbf{J}_{r3} = [\mathbf{0}_{M1 \times p_t} \quad \mathbf{I}_{M1} \quad \mathbf{0}_{M1 \times p_t}] \otimes \mathbf{I}_{N_{\text{sub}}}. \tag{25b}$$

Then the pairing matrix can be written as follows:

$$\mathbf{P}(i, j) = \frac{1}{\left(\dot{\mathbf{a}}_t(\phi_i) \otimes \overline{\mathbf{a}}_r(\theta_j)\right)^{\text{H}} \left(\mathbf{I}_{M_{\text{sub}}N1} - \mathbf{U}_1 \mathbf{U}_1^{\text{H}}\right) \left(\dot{\mathbf{a}}_t(\phi_i) \otimes \overline{\mathbf{a}}_r(\theta_j)\right)} \bullet \frac{1}{\left(\overline{\mathbf{a}}_t(\phi_i) \otimes \dot{\mathbf{a}}_r(\theta_j)\right)^{\text{H}} \left(\mathbf{I}_{M1N_{\text{sub}}} - \mathbf{U}_2 \mathbf{U}_2^{\text{H}}\right) \left(\overline{\mathbf{a}}_t(\phi_i) \otimes \dot{\mathbf{a}}_r(\theta_j)\right)}, \tag{26}$$

where $\mathbf{P}$ is a $P \times P$ matrix. $\dot{\mathbf{a}}_t(\phi_i), \overline{\mathbf{a}}_t(\phi_i)$ are the first $M_{\text{sub}}, M1$ rows of $\mathbf{a}_t(\phi_i)$, respectively. $\dot{\mathbf{a}}_r(\theta_j), \overline{\mathbf{a}}_r(\theta_j)$ are the first $N_{\text{sub}}, N1$ rows of $\mathbf{a}_r(\theta_j)$, respectively. If $\mathbf{P}(i, j)$ is the largest in the ith row, then we pair ϕ_i with θ_j.

3.4. Mutual Coupling Estimation. In order to calibrate the antennas with unknown mutual coupling, the mutual coupling coefficients need to be estimated.

Lemma 1. *For any $M \times 1$ complex vector $\mathbf{x}$ and any $M \times M$ banded complex symmetric Toeplitz matrix $\mathbf{A}$, we have (Lemma 3 in [17])*

$$\mathbf{A} \cdot \mathbf{x} = \mathbf{Q}(\mathbf{x}) \cdot \mathbf{a}, \tag{27}$$

where the $L \times 1$ vector $\mathbf{a}$ is given by

$$a(l) = \mathbf{A}(1, l), \quad l = 1, 2, \ldots, L \tag{28}$$

and L is the highest superdiagonal that is different from zero. The $M \times L$ matrix $\mathbf{Q}(\mathbf{x})$ is given by the sum of the two $M \times L$ following matrices:

$$[\mathbf{W}_1]_{pq} = \begin{cases} \mathbf{x}_{p+q-1}, & p + q \le M + 1 \\ 0, & \textit{otherwise}, \end{cases} \qquad [\mathbf{W}_2]_{pq} = \begin{cases} \mathbf{x}_{p-q+1}, & p \le q \le 2 \\ 0, & \textit{otherwise}. \end{cases} \tag{29}$$

By Lemma 1, we can get

$$\mathbf{C}_t \mathbf{a}_t(\phi) = \mathbf{T}_t(\phi) \mathbf{c}_t, \quad \mathbf{c}_t = \left[1, c_{t1}, c_{t2}, \ldots, c_{tp_t}\right]^{\text{T}}, \tag{30a}$$

$$\mathbf{C}_r \mathbf{a}_r(\theta) = \mathbf{T}_r(\theta) \mathbf{c}_r, \quad \mathbf{c}_r = \left[1, c_{r1}, c_{r2}, \ldots, c_{rp_r}\right]^{\text{T}}. \tag{30b}$$

The steering matrix and the signal subspace own the relationship as follows:

$$\left([\mathbf{C}_t \mathbf{A}_t] \odot \dot{\mathbf{A}}_r\right) \mathbf{T}_3 = \mathbf{J}_{\text{raug}}^{(4)} \left(\mathbf{Q}_{2MN_{\text{sub}}} \mathbf{E}_{\text{raug}}\right) = \mathbf{U}_3, \quad \mathbf{J}_{\text{raug}}^{(4)} = \left[\mathbf{I}_{MN_{\text{sub}}}, \mathbf{0}_{MN_{\text{sub}}}\right], \tag{31}$$

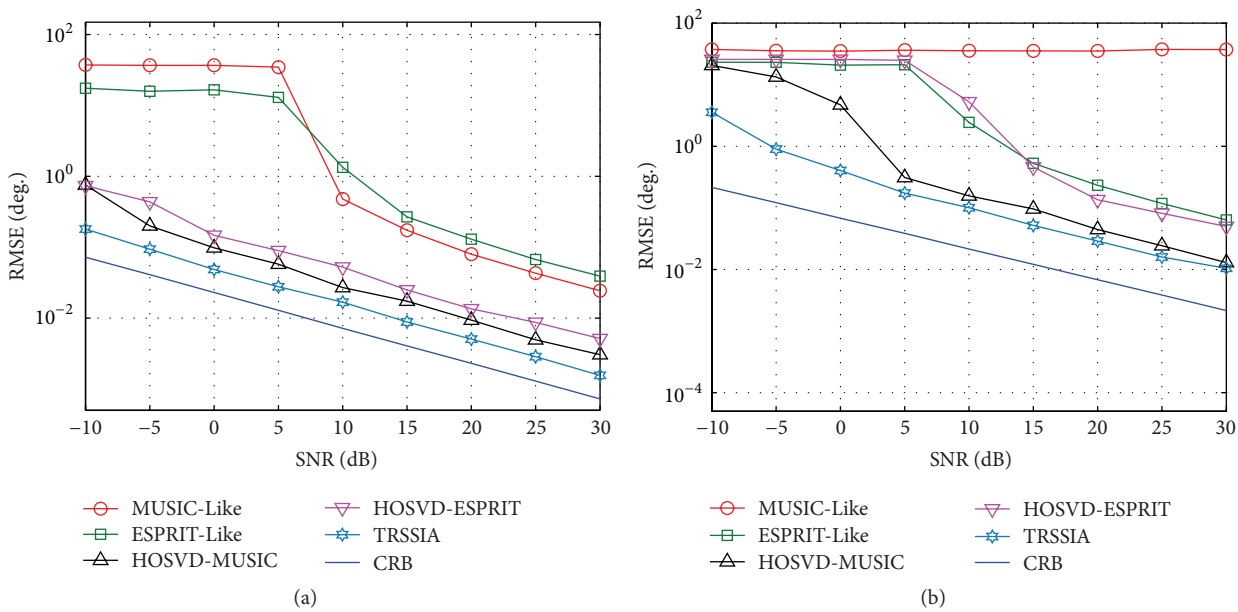

Figure 1: RMSE of angle estimation versus SNR: (a) $P = 3$, $p_t = p_r = 1$, $M_{\text{sub}} = 4$, $N_{\text{sub}} = 4$, $L = 64$ (b) $P = 3$, $p_t = p_r = 2$, $M_{\text{sub}} = 3$, $N_{\text{sub}} = 3$, and $L = 128$.

where $\mathbf{T}_3$ is a $P \times P$ nonsingular matrix. In theory, $\|([\mathbf{C}_t\mathbf{a}_t(\phi_i)] \otimes \dot{\mathbf{a}}_r(\theta_i))^{\text{H}}\mathbf{U}_3^{\perp}\|_2 = 0$, and it also can be written as $\|((\mathbf{T}_t(\phi_i)\mathbf{c}_t) \otimes (\text{diag}(\dot{\mathbf{a}}_r(\theta_i))\mathbf{i}_r)^{\text{H}}\mathbf{U}_3^{\perp}\|_2 = \|(\mathbf{c}_t \otimes \mathbf{i}_r)^{\text{H}}(\mathbf{T}_t(\phi_i) \otimes \text{diag}(\dot{\mathbf{a}}_r(\theta_i)))^{\text{H}}\mathbf{U}_3^{\perp}\|_2 = 0$, where $\mathbf{i}_r$ is a $N_{\text{sub}} \times 1$ vector, whose all elements are ones. $\mathbf{U}_3^{\perp}$ is the orthogonal complement space of $\mathbf{U}_3$. Then the mutual coupling coefficients in transmitter can be obtained as

$$\mathbf{c}_{\text{taug}} = \mathbf{c}_t \otimes \mathbf{i}_r = \mathbf{e}_{\min}\left(\frac{1}{P}\sum_{i=1}^{P}\mathbf{Q}_{ti}\right), \tag{32}$$

where $\mathbf{Q}_{ti} = (\mathbf{T}_t(\phi_i) \otimes \text{diag}(\dot{\mathbf{a}}_r(\theta_i)))^{\text{H}}(\mathbf{I}_{MN_{\text{sub}}} - \mathbf{U}_3^{\text{H}}\mathbf{U}_3)(\mathbf{T}_t(\phi_i) \otimes \text{diag}(\dot{\mathbf{a}}_r(\theta_i)))$. By exploiting the structure of $\mathbf{c}_{\text{taug}}$, we get a matrix $\widetilde{\mathbf{C}}_t = \text{mat}(\mathbf{c}_{\text{taug}}) = \mathbf{c}_t\mathbf{i}_r^{\text{T}}$. Then the estimated mutual coupling coefficient can be obtained with the operations:

$$\begin{aligned} &\widetilde{\mathbf{C}}_t(1, :) = \mathbf{i}_r^{\text{T}}, \\ &\{\widehat{c}_{ti}\}_{i=1}^{p_t} = \text{mean}\left(\widetilde{\mathbf{C}}_t(i+1, :)\right). \end{aligned} \tag{33}$$

The mutual coupling coefficients in receiver also can be figured out in the same way. By exploiting the relationship between steering matrix and signal subspace $(\dot{\mathbf{A}}_t \odot [\mathbf{C}_r\mathbf{A}_r])\mathbf{T}_4 = \mathbf{J}_{\text{taug}}^{(4)}(\mathbf{Q}_{2M_{\text{sub}}N}\mathbf{E}_{\text{taug}}) = \mathbf{U}_4$, where $\mathbf{J}_{\text{taug}}^{(4)} = [\mathbf{I}_{M_{\text{sub}}N}, \mathbf{0}_{M_{\text{sub}}N}]$. The vector $\mathbf{c}_{\text{raug}}$ can be obtained and the estimated mutual coupling coefficients can be obtained by $\{\widehat{c}_{rj}\}_{j=1}^{p_r} = \text{mean}(\widetilde{\mathbf{C}}_r(j+1, :))$.

4. Simulation Results

In the following simulations, we assume that both the transmit and receive arrays are ULAs with $M = 10$ and $N = 10$ and d_t and d_r are both half wavelength. The transmitter emits the orthogonal waveforms $\widetilde{\mathbf{S}} = (1 + j)\mathbf{H}/\sqrt{2}$, where $\mathbf{H} \in \mathbb{C}^{M\times K}$ is constructed with M rows of a $K \times K$ Hadamard matrix and $K = 256$. There are three targets at the same range bin with RCS $\beta = [1, 1, 1]^{\text{T}}$ and the Doppler frequencies $\mathbf{f}_d = [100, 255, 500]^{\text{T}}$ Hz. And these targets locate at $(\phi_1, \theta_1) = (-15^\circ, 40^\circ)$, $(\phi_2, \theta_2) = (35^\circ, -20^\circ)$, and $(\phi_3, \theta_3) = (0^\circ, -10^\circ)$. All the simulation results are carried out by 100 Monte Carlo trials in this paper.

In the first simulation, we investigate the angle estimation performances of MUSIC-Like, ESPRIT-Like, and tensor-based real-valued subspace (in this paper, we call it HOSVD) methods and our proposed TRSSIA method. There are two cases: (1) $p_t = p_r = 1$, $\mathbf{c}_t = [1, 0.2 + j0.0061]^{\text{T}}$, and $\mathbf{c}_r = [1, 0.15 + j0.0251]^{\text{T}}$: the number of pulses is $L = 64$; and (2) $p_t = p_r = 2$, $\mathbf{c}_t = [1, 0.7 + j0.002, 0.2 + j0.0061]^{\text{T}}$, and $\mathbf{c}_r = [1, 0.6 + j0.0121, 0.15 + j0.0251]^{\text{T}}$: the number of pulses is $L = 128$. In Figure 1(a), it shows that TRSSIA estimates angles with more accuracy than the other approaches. The MUSIC-Like and ESPRIT-Like methods perform well in the high SNR region for case (1), as shown in Figure 1(b), and MUSIC-Like fails to work in case (2) owing to angle ambiguity, which is explained in [13]. At both cases, the TRSSIA method is better than the other methods. Although the HOSVD methods make use of the multidimensional structure of the received data, it just selects $M - 2p_t$ elements of transmit array and $N - 2p_r$ elements of receive array for angles estimation. The TRSSIA algorithm restrains the noise of received data, improves the effective aperture, and uses all the elements of transmitter and receiver.

The second simulation is carried out to show the RMSE of angle estimation versus number of pulses with SNR = 5 dB. Figure 2(a) shows that the performances of MUSIC-Like and ESPRIT-Like approaches highly depend on the number of

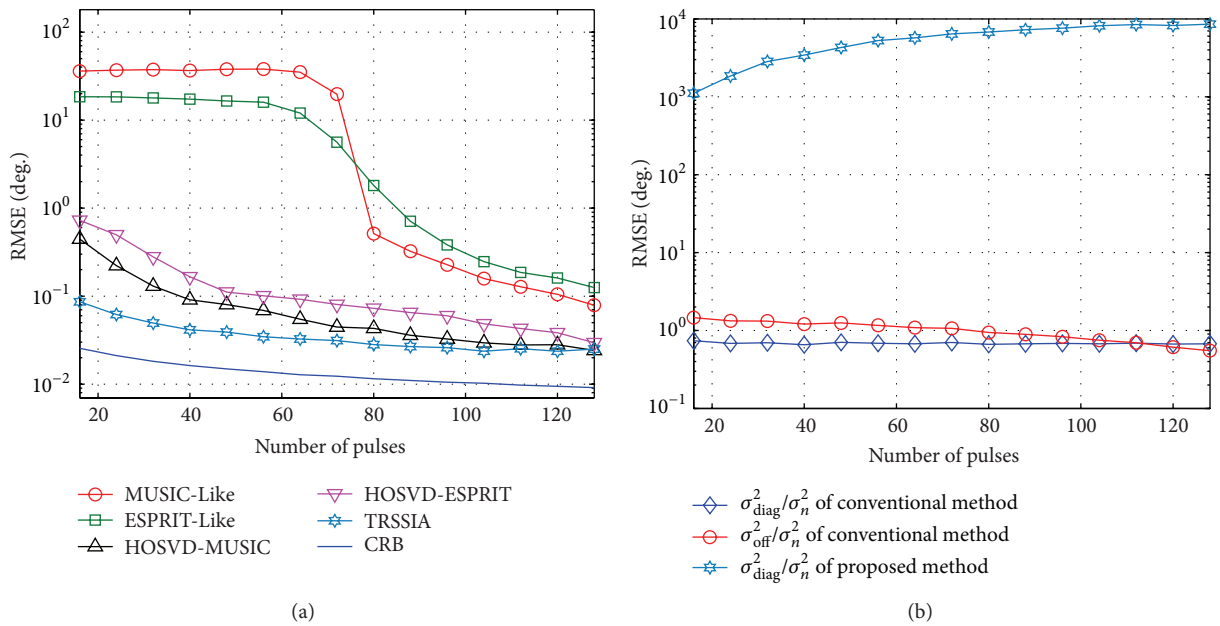

FIGURE 2: (a) RMSE of angle estimation versus number of pulses. (b) The ratio of signal power to noise power versus number of pulses ($P = 3$, $p_t = p_r = 1$, $M_{\text{sub}} = 4$, $N_{\text{sub}} = 4$, and SNR = 5 dB).

pulses, and the TRSSIA method can give out more precise angle estimation even with small snapshots. In Figure 2(b), it analyses the ratio of the power of signal to the power of noise. σ^2_{diag}, σ^2_{off}, and σ^2_n represent the sum of diagonal elements of autocorrelation matrix of signal, the sum of off-diagonal elements of autocorrelation matrix of signal, and the sum of all elements of autocorrelation matrix of noise, respectively. In our proposed algorithm, the newly autocorrelation matrices of signal are $\widehat{\Lambda}_t$ and $\widehat{\Lambda}_r$. For the other methods, we call them conventional methods; it is $\sum_{l=1}^{L} \mathbf{s}(l)\mathbf{s}(l)^{\text{H}}/L$. According to (1), the σ^2_{off} of the TRSSIA method is zero. Because the TRSSIA method restrains the noise, the $\sigma^2_{\text{diag}}/\sigma^2_n$ is tremendously higher than conventional methods. Though the $\sigma^2_{\text{diag}}/\sigma^2_n$ of conventional methods is constant, the $\sigma^2_{\text{off}}/\sigma^2_n$ gets lower as the number of pulses increases, which improves the accuracy of signal subspace estimation and angle estimation.

In the third simulation, it compares the angle estimation performance of the TRSSIA method with the performance of the HOSVD methods in the scenario of coherent targets. There are three cases: (1) $\mathbf{f}_d = [100, 110, 200]^{\text{T}}$ Hz; (2) $\mathbf{f}_d = [100, 100, 150]^{\text{T}}$ Hz; and (3) $\mathbf{f}_d = [100, 100, 100]^{\text{T}}$ Hz. As Figure 3 shows, the angle estimation performance of the HOSVD methods degrade, when all the targets move in a narrow speed zone. This method even cannot work when more than two coherent targets exist. Equation (1) proves that the rank is always P whether the targets are coherent or not, so the angle estimation performance of the TRSSIA method does not degrade even if there are more than two coherent targets.

As we know, the forward-backward (FB) smoothing is a preferable technique to cope with coherent signals [23]. It should be notable that our proposed approach can perform as well as the joint transmit and receive diversity smoothing

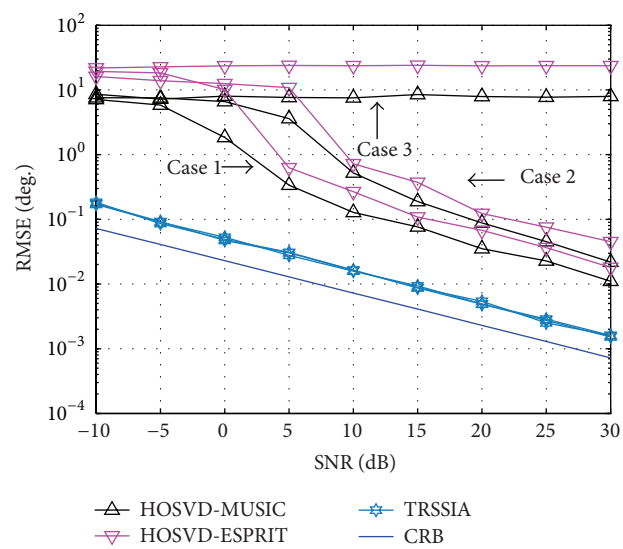

FIGURE 3: RMSE of angle estimation versus SNR with coherent targets ($P = 3$, $p_t = p_r = 1$, $M_{\text{sub}} = 4$, $N_{\text{sub}} = 4$, and $L = 64$).

(TRDS) algorithm with FB smoothing in [24], as it is shown in Figure 4(a). But the TRSSIA needs to compute covariance matrices only once. We present an evaluation of computational complexity using TIC and TOC instruction in MATLAB. In Figure 4(b), it demonstrates that the runtime gap between two methods gets wider with the number of pulses increasing.

The performance of mutual coupling estimation is demonstrated in the fourth simulation. The RMSEs of the real part and the imaginary part of mutual coupling are adapted

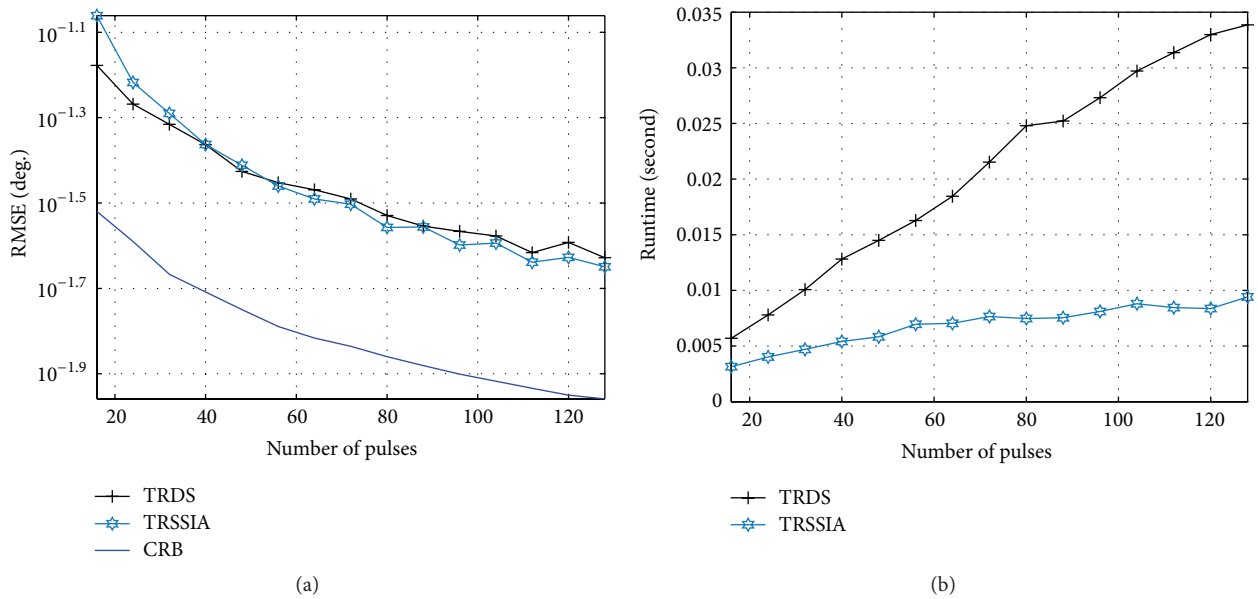

FIGURE 4: (a) RMSE of angle estimation versus number of pulses with coherent targets. (b) Runtime of both TRDS and TRSSIA algorithms versus number of pulses ($P = 3$, $f_d = [100, 100, 100]$ Hz, $p_t = p_r = 1$, SNR = 5 dB; TRDS: $M_{\text{sub}} = 5$, $N_{\text{sub}} = 5$; TRSSIA: $M_{\text{sub}} = 4$, $N_{\text{sub}} = 4$).

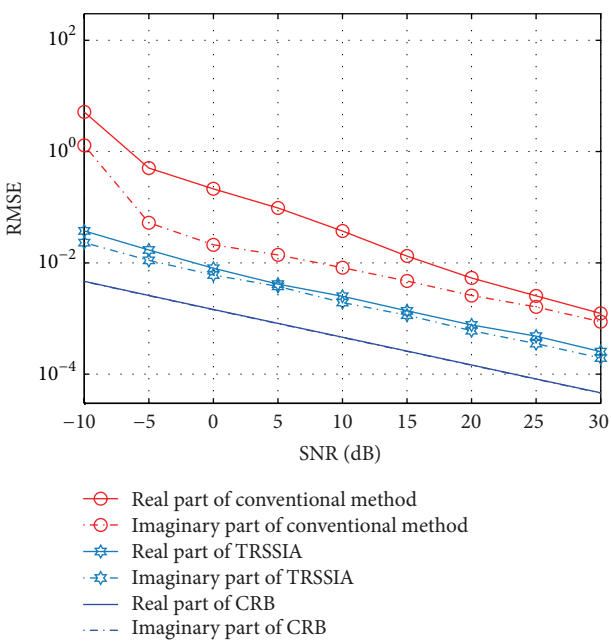

FIGURE 5: RMSE of mutual coupling estimation versus SNR ($P = 3$, $p_t = p_r = 1$, $M_{\text{sub}} = 4$, $N_{\text{sub}} = 4$, and $L = 64$).

to measure the performance. In [13, 14], a technique of estimating mutual coupling is proposed; we call it conventional method in this paper. Figure 5 shows that our proposed approach can estimate mutual coupling more accurately. There are two reasons. On one hand, the angle estimation of our proposed method is more accurate. On the other hand, our proposed method computes the mean of every mutual coupling coefficient.

5. Conclusion

This paper has proposed an algorithm for angle estimation with unknown mutual coupling in both the transmitter and receiver. The preliminary work is to restrain the white Gaussian noise of each channel by computing the correlation coefficients, because the noise is independent in both the spatial and temporal domains. In order to use more information of the received data, we do spatial smoothing in both the transmit array and the receive array and construct the augmented steering matrices with improved aperture. The TRSSIA algorithm adopts more elements from the transmitter and the receiver to estimate angles. So more information improves the angle estimation. For restraining noise, improving aperture and the spatial smoothing technique, the TRSSIA method proves better angle estimation than MUSIC-Like, ESPRIT-Like, and tensor-based real-valued approaches at small number of pulses and low SNR cases, and its angle estimation performance does not descend even for more than two coherent targets. Based on the more accurately estimated angles and computing the mean of every mutual coupling efficient, the mutual coupling estimation is more accurate than the other methods. The simulation results verify the advantage of the proposed method.

Appendix

Rotational Invariance Property of $\widehat{\mathbf{X}}_{\text{taug}}$

Firstly, we do SVD on $\widehat{\mathbf{X}}_{\text{taug}}$ and get P major left eigenvectors, which can be expressed as $\mathbf{U}_{TS} \in \mathbb{C}^{2M_{\text{sub}}N\times P}$. And the relationship between $\mathbf{U}_{TS}$ and $\mathbf{A}_{\text{taug}}$ is $\mathbf{U}_{TS} = \mathbf{A}_{\text{taug}}\mathbf{T}$, where $\mathbf{T}$ is an nonsingular matrix of $P \times P$ dimensions. We equally divide $\mathbf{U}_{TS}$ into two parts; $\overline{\mathbf{U}}_{TS}$ and $\underline{\mathbf{U}}_{TS}$ mean the first and last

$M_{\text{sub}}N$ rows of $\mathbf{U}_{TS}$, respectively. Then the above equation can be written as

$$\begin{bmatrix} \overline{\mathbf{U}}_{TS} \\ \underline{\mathbf{U}}_{TS} \end{bmatrix} = \begin{bmatrix} \dot{\mathbf{A}}_t \odot \widetilde{\mathbf{A}}_r \widehat{\mathbf{\Lambda}}_t \\ \dot{\mathbf{A}}_t \odot \left(\mathbf{\Pi}_N \widetilde{\mathbf{A}}_r^*\right) \mathbf{\Lambda}_{t1} \widehat{\mathbf{\Lambda}}_t^* \mathbf{\Lambda}_{t2} \end{bmatrix} \mathbf{T}. \tag{A.1}$$

Then we explore the rotational invariance of $\dot{\mathbf{A}}_t$,

$$\begin{aligned} &\overline{\dot{\mathbf{A}}}_t \odot \widetilde{\mathbf{A}}_r \widehat{\mathbf{\Lambda}}_t \mathbf{T} = \overline{\mathbf{U}}_{TS1} = \overline{\mathbf{U}}_{TS}\left[1 : \left(M_{\text{sub}} - 1\right) N, :\right], \\ &\underline{\dot{\mathbf{A}}}_t \odot \widetilde{\mathbf{A}}_r \widehat{\mathbf{\Lambda}}_t \mathbf{T} = \overline{\mathbf{U}}_{TS2} = \overline{\mathbf{U}}_{TS}\left[N + 1 : M_{\text{sub}} N, :\right], \\ &\overline{\dot{\mathbf{A}}}_t \odot \left(\mathbf{\Phi}_N \widetilde{\mathbf{A}}_r^*\right) \mathbf{\Lambda}_{t1} \widehat{\mathbf{\Lambda}}_t^* \mathbf{\Lambda}_{t2} \mathbf{T} = \underline{\mathbf{U}}_{TS1} \\ &\quad = \underline{\mathbf{U}}_{TS}\left[1 : \left(M_{\text{sub}} - 1\right) N, :\right], \\ &\underline{\dot{\mathbf{A}}}_t \odot \left(\mathbf{\Phi}_N \widetilde{\mathbf{A}}_r^*\right) \mathbf{\Lambda}_{t1} \widehat{\mathbf{\Lambda}}_t^* \mathbf{\Lambda}_{t2} \mathbf{T} = \underline{\mathbf{U}}_{TS2} \\ &\quad = \underline{\mathbf{U}}_{TS}\left[N + 1 : M_{\text{sub}} N, :\right] \end{aligned} \tag{A.2}$$

and these matrices meet $\overline{\dot{\mathbf{A}}}_t \mathbf{\Phi}_t = \underline{\dot{\mathbf{A}}}_t$, where $\overline{\dot{\mathbf{A}}}_t$ and $\underline{\dot{\mathbf{A}}}_t$ are the first and last $M_{\text{sub}} - 1$ rows of $\dot{\mathbf{A}}_t$, $\mathbf{\Phi}_t = \text{diag}([\exp(\text{j}2\pi d_t \sin\phi_1/\lambda), \ldots, \exp(\text{j}2\pi d_t \sin\phi_p/\lambda)])$. Thus, the rotational invariance of $\mathbf{A}_{\text{taug}}$ can be shown in the following equation:

$$\begin{aligned} &\begin{bmatrix} \overline{\dot{\mathbf{A}}}_t \odot \widetilde{\mathbf{A}}_r \widehat{\mathbf{\Lambda}}_t \\ \overline{\dot{\mathbf{A}}}_t \odot \left(\mathbf{\Phi}_N \widetilde{\mathbf{A}}_r^*\right) \mathbf{\Lambda}_{t1} \widehat{\mathbf{\Lambda}}_t^* \mathbf{\Lambda}_{t2} \end{bmatrix} \mathbf{\Phi}_t \\ &\quad = \begin{bmatrix} \underline{\dot{\mathbf{A}}}_t \odot \widetilde{\mathbf{A}}_r \widehat{\mathbf{\Lambda}}_t \\ \underline{\dot{\mathbf{A}}}_t \odot \left(\mathbf{\Phi}_N \widetilde{\mathbf{A}}_r^*\right) \mathbf{\Lambda}_{t1} \widehat{\mathbf{\Lambda}}_t^* \mathbf{\Lambda}_{t2} \end{bmatrix} \Longrightarrow \\ &\begin{bmatrix} \overline{\mathbf{U}}_{TS1} \\ \underline{\mathbf{U}}_{TS1} \end{bmatrix}^{\dagger} \begin{bmatrix} \overline{\mathbf{U}}_{TS2} \\ \underline{\mathbf{U}}_{TS2} \end{bmatrix} = \mathbf{T}^{-1} \mathbf{\Phi}_t \mathbf{T}. \end{aligned} \tag{A.3}$$

Then EVD can be employed to solve $\mathbf{\Phi}_t$; furthermore, DOD can be got. The above deducing procedure proves the rotational invariance property of $\mathbf{X}_{\text{taug}}$.

Conflict of Interests

The authors declare that there is no conflict of interests regarding the publication of this paper.

References

[1] D. W. Bliss and K. W. Forsythe, "Multiple-input multiple-output (MIMO) radar and imaging: degrees of freedom and resolution," in *Proceedings of the Conference Record of the 37th IEEE Asilomar Conference on Signals, Systems and Computers (ACSSC '03)*, vol. 1, pp. 54–59, Pacific Grove, Calif, USA, November 2003.

[2] E. Fishler, A. Haimovich, R. Blum, D. Chizhik, L. Cimini, and R. Valenzuela, "MIMO radar: an idea whose time has come," in *Proceedings of the IEEE Radar Conference*, pp. 71–78, April 2004.

[3] E. Fishler, A. Haimovich, R. Blum, R. Cimini, D. Chizhik, and R. Valenzuela, "Performance of MIMO radar systems: advantages of angular diversity," in *Proceedings of the 38th IEEE Asilomar Conference on Signals, Systems and Computers*, vol. 1, pp. 305–309, IEEE, Pacific Grove, Calif, USA, November 2004.

[4] A. Farina and M. Lesturgation, "Guest editorial: special issue on bistatic and MIMO radars and their applications in surveillance and remote sensing," *IET Radar, Sonar and Navigation*, vol. 8, no. 2, pp. 73–74, 2014.

[5] A. M. Haimovich, R. S. Blum, and L. J. Cimini, "MIMO radar with widely separated antennas," *IEEE Signal Processing Magazine*, vol. 25, no. 1, pp. 116–129, 2008.

[6] J. Li and P. Stoica, "MIMO radar with colocated antennas," *IEEE Signal Processing Magazine*, vol. 24, no. 5, pp. 106–114, 2007.

[7] H. Yan, J. Li, and G. Liao, "Multitarget identification and localization using bistatic MIMO radar systems," *EURASIP Journal on Advances in Signal Processing*, vol. 2008, Article ID 283483, 8 pages, 2008.

[8] D. Chen, B. Chen, and G. Qin, "Angle estimation using ESPRIT in MIMO radar," *Electronics Letters*, vol. 44, no. 12, pp. 770–771, 2008.

[9] G. Zheng, B. Chen, and M. Yang, "Unitary ESPRIT algorithm for bistatic MIMO radar," *Electronics Letters*, vol. 48, no. 3, pp. 179–181, 2012.

[10] X. Zhang, L. Xu, L. Xu, and D. Xu, "Direction of Departure (DOD) and Direction of Arrival (DOA) estimation in MIMO radar with reduced-dimension MUSIC," *IEEE Communications Letters*, vol. 14, no. 12, pp. 1161–1163, 2010.

[11] D. Nion and N. D. Sidiropoulos, "Tensor algebra and multidimensional harmonic retrieval in signal processing for MIMO radar," *IEEE Transactions on Signal Processing*, vol. 58, no. 11, pp. 5693–5705, 2010.

[12] L. Constancias, M. Cattenoz, P. Brouard, and A. Brun, "Coherent collocated MIMO radar demonstration for air defence applications," in *Proceedings of the IEEE Radar Conference (RADAR '13)*, pp. 1–6, Ottawa, Canada, April-May 2013.

[13] X. Liu and G. Liao, "Direction finding and mutual coupling estimation for bistatic MIMO radar," *Signal Processing*, vol. 92, no. 2, pp. 517–522, 2012.

[14] Z. Zheng, J. Zhang, and J. Zhang, "Joint DOD and DOA estimation of bistatic MIMO radar in the presence of unknown mutual coupling," *Signal Processing*, vol. 92, no. 12, pp. 3039–3048, 2012.

[15] X. Wang, W. Wang, J. Liu, Q. Liu, and B. Wang, "Tensor-based real-valued subspace approach for angle estimation in bistatic MIMO radar with unknown mutual coupling," *Signal Processing*, vol. 116, pp. 152–158, 2015.

[16] A. Thakre, M. Haardt, and K. Giridhar, "Single snapshot spatial smoothing with improved effective array aperture," *IEEE Signal Processing Letters*, vol. 16, no. 6, pp. 505–508, 2009.

[17] B. Friedlander and A. J. Weiss, "Direction finding in the presence of mutual coupling," *IEEE Transactions on Antennas and Propagation*, pp. 273–284, 1991.

[18] F. Gao, B. Jiang, X. Gao, and X.-D. Zhang, "Superimposed training based channel estimation for OFDM modulated amplify-and-forward relay networks," *IEEE Transactions on Communications*, vol. 59, no. 7, pp. 2029–2039, 2011.

[19] G. Wang, F. Gao, W. Chen, and C. Tellambura, "Channel estimation and training design for two-way relay networks in time-selective fading environments," *IEEE Transactions on Wireless Communications*, vol. 10, no. 8, pp. 2681–2691, 2011.

[20] X. Zhang, *Matrix Analysis and Applications*, Tsinghua University Press, Beijing, China, 2013.

[21] F. Roemer, M. Haardt, and G. Del Galdo, "Analytical performance assessment of multi-dimensional matrix- and tensor-based ESPRIT-type algorithms," *IEEE Transactions on Signal Processing*, vol. 62, no. 10, pp. 2611–2625, 2014.

[22] M. Haardt and J. A. Nossek, "Unitary ESPRIT: how to obtain increased estimation accuracy with a reduced computational burden," *IEEE Transactions on Signal Processing*, vol. 43, no. 5, pp. 1232–1242, 1995.

[23] L. Zhang, W. Liu, and L. Yu, "Performance analysis for finite sample MVDR beamformer with forward backward processing," *IEEE Transactions on Signal Processing*, vol. 59, no. 5, pp. 2427–2431, 2011.

[24] W. Zhang, W. Liu, J. Wang, and S. L. Wu, "Joint transmission and reception diversity smoothing for direction finding of coherent targets in MIMO radar," *IEEE Journal on Selected Topics in Signal Processing*, vol. 8, no. 1, pp. 115–124, 2014.

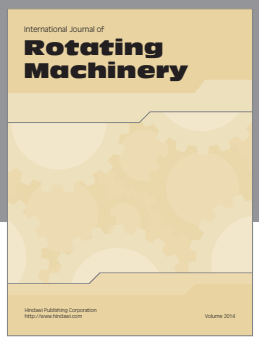

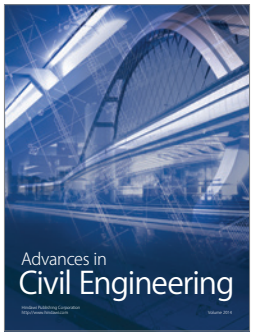

Hindawi
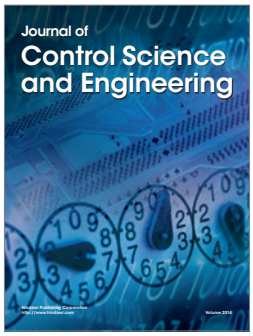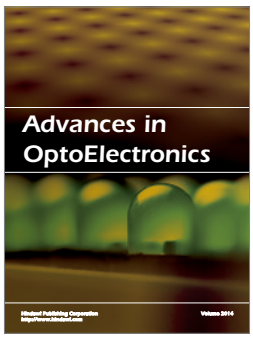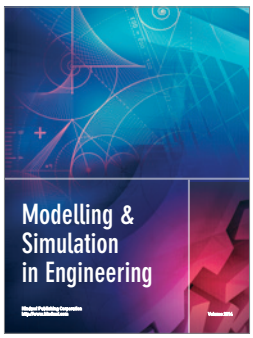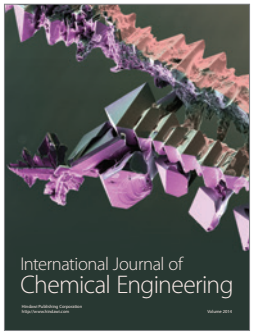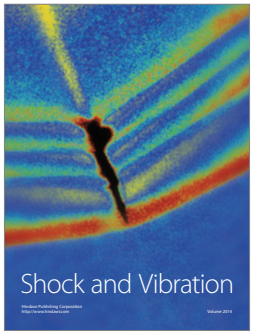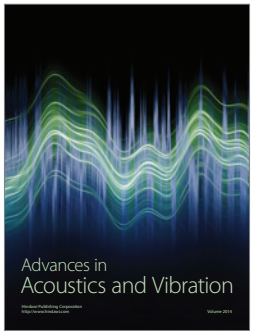
Submit your manuscripts at
http://www.hindawi.com